Journal of Applied Pharmaceutical Science Vol. 15(08), pp 071-081, August, 2025
Available online at http://www.japsonline.com
DOI: 10.7324/JAPS.2025.230314
ISSN 2231-3354

Green synthesis of zinc oxide nanoparticles using ethyl acetate fraction of white frangipani leaves (*Plumeria alba* L.) and its application as antidandruff shampoo

Dian Riana Ningsih*, Putri Caroline, Purwati Purwati, Zusfahair Zusfahair, Anung Riapanitra
Department of Chemistry, Jenderal Soedirman University, Purwokerto, Indonesia.

ARTICLE HISTORY
Received on: 09/01/2025
Accepted on: 19/04/2025
Available Online: 05/07/2025

Key words:
Ethyl acetate, *P. alba* L., *S. aureus,* Shampoo, ZnO-NPs.

ABSTRACT

Dandruff and seborrheic dermatitis are scalp conditions caused by the body's natural microorganisms. Shampoo serves as an alternative solution by removing impurities and inhibiting microbial growth. The ethyl acetate fraction of white frangipani leaves (*Plumeria alba L.*) exhibits antibacterial properties due to its secondary metabolite compounds. Zinc oxide nanoparticles (ZnO-NPs) possess antibacterial activity and are safe for use on human skin. This study aims to develop an antidandruff shampoo formulation by incorporating ZnO-NPs synthesized with ethyl acetate fraction. Processes involved include the extraction and fractionation, synthesis and characterization of ZnO-NPs, formulation and characterization of ZnO-NPs shampoo, and antibacterial activity test against *Staphylococcus aureus*. Ethanol extract yield was 15.14%, n-hexane fraction was 15.11%, ethyl acetate fraction was 8.83%, and the ethanol fraction was 53.77%. The antibacterial activity test showed that the ethyl acetate fraction exhibited the highest inhibition diameter at 1.81 ± 0.42 mm. Phytochemical tests revealed that the fraction contains polyphenols, flavonoids, saponins, alkaloids, and terpenoids. ZnO-NPs with optimal antibacterial activity were obtained using 0.15-M *P. alba* ZnO-NPs, which were then formulated and characterized into a nanoparticle shampoo. Based on the study, 0.15-M *P. alba* ZnO-NPs shampoo formulation effectively inhibited bacterial growth and demonstrated stability in the shampoo formulation.

INTRODUCTION

Dandruff and seborrheic dermatitis are scalp disorders caused by excessive secretion of sweat glands and presence of microorganisms such as *Staphylococcus aureus*, *Streptococcus*, and *Pityrosporum ovale* [1]. Related to point three of UNSDGs, the development of natural resources to minimize dandruff and seborrheic dermatitis on scalp could have a positive impact on people's good health and well-being. These issues can be addressed using antidandruff shampoos. However, prolonged use of such shampoos can lead to scalp damage, highlighting the need for exploring active compounds derived from natural sources. White Frangipani (*P. alba* L.) is a species of frangipani (*Plumeria*) that grows vastly in Indonesia and has potential as an herbal plant [2]. Based on [3], 30-ppm ethanol extract of white frangipani leaves could inhibit the growth of *S. aureus* and *P. ovale.* The ability of white frangipani leaves to inhibit the growth of *S. aureus* and *P. ovale* is due to secondary metabolite compounds, such as alkaloids and saponins. Secondary metabolite compounds penetrate the cell wall to inhibit microbial growth. Exploration of white frangipani leaves (*P. alba* L.) needs to be conducted to improve the inhibition of antimicrobial activity, such as the synthesis of the white frangipani leaves extract (*P. alba* L.) with nanotechnology [4].

Green synthesis is a bottom-up approach to nanoparticle synthesis, similar to the chemical nanoparticle synthesis method. However, the expensive chemical reducing agents used in chemical synthesis are replaced with natural extracts, such as those derived from leaves or fruits, for the synthesis of metals or metal oxides. Natural extracts have

*Corresponding Author
Dian Riana Ningsih, Department of Chemistry, Jenderal Soedirman University, Purwokerto, Indonesia. E-mail: dian.ningsih @ unsoed.ac.id

good potential for producing nanoparticles. These biological materials, used as bioreductants in nanoparticle synthesis, have been proven to be environmentally friendly, sustainable, free from chemical contamination, more cost-effective, and suitable for large-scale production [5]. Besides that, the trend of the "back to nature" issue increasingly encourages optimizing natural material utilization.

Zinc oxide (ZnO) is a white powder compound naturally found as the mineral zincite [6]. Its hardness, stiffness, and piezoelectric constant make ZnO an important material in the ceramics industry. Additionally, its low toxicity, biocompatibility, and biodegradability make ZnO suitable for biomedical applications and eco-friendly systems [7]. ZnO versatility allows it to be utilized in a wide range of applications, such as antimicrobial photocatalysis and water purification [8].

Synthesis of zinc oxide nanoparticles (ZnO-NPs) using ethyl acetate fraction of white frangipani leaves (*P. alba* L.) needs to be researched for obtaining the inhibition rate of *S. aureus* and *P. ovale* as antidandruff shampoo ingredients. ZnO-NPs were chosen because they have good antimicrobial activity and are harmless [8]. Based on the explanation above, the synthesis of zinc oxide nanoparticles using ethyl acetate fraction of white frangipani leaves (*P. alba* L.) will be held and tested for antimicrobial activity against *S. aureus* and *P. ovale*. Furthermore, the synthesized ZnO-NPs were characterized using techniques such as Fourier transform infrared (FTIR), X-ray diffraction (XRD), particle size analyzer (PSA), and scanning electron microscope-energy-dispersive X-ray (SEM-EDX). ZnO-NPs will be formulated as antidandruff shampoo and tested to *S. aureus*.

MATERIALS AND METHODS

Tools and materials

Equipment used in this study included incubator, autoclave, centrifuges, blender, pH meter, vacuum rotary evaporator, analytical balance, furnace, UV-Vis spectrophotometer, FTIR spectroscopy system (IRPrestige-21 SHIMADZU), XRD system (PANalytical X'Pert3), PSA system (Microtrac Flex 11 Software Operations Manual), SEM-EDX system (JEOL JSM-6510LA), filler, volumetric pipette, watch glass, microscope slides, magnetic stirrer, porcelain crucibles, micropipette, biosafety cabinet-type ESCO Class II, stirring rods, Bunsen burner, beakers (Pyrex), test tubes, Erlenmeyer flasks, calipers, Petri dishes, funnels, measuring cylinders (Pyrex), spatulas, spirit lamp, inoculating needle, cork borer, separatory funnel, dilution flask, rubber, gauze, cotton, filter paper, drugal sky, and wrapping materials.

White frangipani leaves (*P. alba* L.), ethanol, n-hexane, ethyl acetate, $FeCl_3$, HCl, NaCl, H_2SO_4, magnesium, $Zn(CH_3COO)_2 \cdot 2H_2O$, NaOH, distilled water, *S. aureus* and *P. ovale* bacterial isolate, nutrient agar (NA), nutrient broth, and 70% alcohol. All materials were obtained from Jenderal Soedirman University, Indonesia.

Study procedure

Extraction and fractionation of white frangipani leaves

White frangipani leaves were washed, dried, ground, and sieved. A total of 300 g of white frangipani (*P. alba* L.) leaf powder was macerated in ethanol for 24 hours. The mixture was then filtered to obtain the filtrate and residue. The residue was repeatedly macerated until the fifth filtrate was collected and evaporated using a rotary evaporator at 80°C. The concentrated ethanol extract was fractionated using n-hexane, ethyl acetate, and ethanol as solvents through liquid–liquid partitioning. The fractions were then concentrated using a rotary evaporator [3].

Antimicrobial activity test of extract and fraction of white frangipani leaves

Antimicrobial activity was assessed using the agar well diffusion method. The study employed bacterial strains *S. aureus* and *P. ovale*. To carry out the procedure, one dose of bacteria was incubated in 10 ml nutrient broth for 24 hours at 37˚C. Bacterial cultures were streaked onto the media, and 6-mm wells were created using a cork borer. Subsequently, each well was filled with 50 µl of frangipani leaf extract and incubated at 37°C for 24 hours [3].

Phytochemical test of ethyl acetate fraction of white frangipani leaves

Ethanol extract of white frangipani leaves (*P. alba* L.) with the highest antibacterial activity was subjected to the phytochemical test to identify active compounds [9]. In the polyphenols test, ethyl acetate fraction of white frangipani leaves heated with 2.5% tween 80 and filtered, and 3 drops of $FeCl_3$ were added. The presence of polyphenol turned the solution into green, red violet, blue, or strong black [10]. In the flavonoids test, the fraction of ethyl acetate diluted with 2.5% tween 80, magnesium powder, and concentrated HCl was added [11]. Color change to yellow indicates flavonoids. In the tannins test, to 5 ml of heated extract, 1 ml of NaCl 2% and 5 ml of gelatin solution were added. The presence of precipitate indicated the presence of tannins. In the saponins test, ethyl acetate fraction in a test tube was mixed with 10 ml of distilled water, shaken, left to stand upright for 30 minutes, and then added with dilute HCl. The persistence of foam indicates the presence of saponins [12]. In the alkaloid test, a total of 10 ml of 1% HCl was added to the ethyl acetate fraction and heated for 10 minutes. The filtered suspension was then treated with 3 drops of Mayer's reagent. The formation of a precipitate in the solution indicates the presence of alkaloids. In the steroids/terpenoids test, anhydrous acetic acid and concentrated H_2SO_4 were added to the ethyl acetate fraction. A green–blue color change indicates the presence of steroids, but if the color changes to red–brown purple, it indicates the presence of triterpenoids [9].

Synthesis of zinc oxide nanoparticles

A total of 90 ml of $Zn(CH_3COO)_2 \cdot 2H_2O$ solution was added to 10 ml of white frangipani leaf ethyl acetate fraction as a precursor. The precursor varied at concentrations of 0.05, 0.10, and 0.15 M. The solution was heated at 70°C for 1 hour, adjusted to a pH of 7, and stirred continuously for 1 hour. The resulting nanoparticle formed a white colloid as shown in Figure 1. Centrifuged at 4,000 rpm for 10 minutes, washed with deionized water, and dried in an oven at 100°C overnight. Pure ZnO-NPs were obtained through a calcination process. Solid material was placed in a furnace at 400°C for 4 hours.

Antimicrobial activity test of zinc oxide nanoparticles and data analysis

Antibacterial activity was tested using the well diffusion method. Testing was carried out on ZnO-NPs with concentration variations of 0.05 M, 0.10 M, and 0.15 M. Testing the antibacterial activity of ZnO-NPs also used the antibacterial activity test method previously.

Data analysis was held by using SPSS and began with testing the data using the Shapiro–Wilk method, while the homogeneity test was held by using Lavene's test. Data that fulfilled the normality assumption and homogeneity were tested by using one-way ANOVA to test the significance of difference between groups with p-value < 0.05. If the test showed a significant difference, the analysis continued with post hoc Duncan to compare the groups more specifically.

Characterization of zinc oxide nanoparticles

ZnO-NPs 0.15-M *P. Alba* as Np-ZnO with the highest antibacterial activity was analyzed using FTIR and scanning electron microscope-energy-dispersive X-ray at the Integrated Research and Testing Laboratory of Gadjah Mada University, XRD at the Materials and Metallurgy Laboratory of Sepuluh Nopember Institute of Technology, and PSA at the Materials Physics Laboratory of Negeri Yogyakarta University.

Formulation and characterization of antidandruff shampoo

Antidandruff shampoo formulation followed the method in [13] with modification. The shampoo formulation was prepared by heating 50 ml of distilled water, adding 10 g of SLS, and stirring until homogeneous. Then, 4 g of cocamide DEA and 0.2 g of propylparaben, dissolved in a few drops of ethanol, were added to the mixture. Once the mixture was homogeneous, the volume of CMC and 0.15-M ZnO-NPs was varied by adding 1 ml, 5 ml, and 10 ml from a 1,000-ppm stock solution. The mixture was stirred until homogeneous, and citric acid was added to adjust the pH to approximately 6.3 while stirring. Menthol dissolved in ethanol was then added. Finally, distilled water was added to the mixture to reach a total volume of 80 ml. The same procedure was applied to the positive and negative controls. The composition of formulation is shown in Table 1. Shampoo formulation was then characterized in terms of acidity, water content, free alkali (SNI 06-2692-1992), emulsion stability following [14], foam stability following [15], and viscosity parameter also tested based on [16].

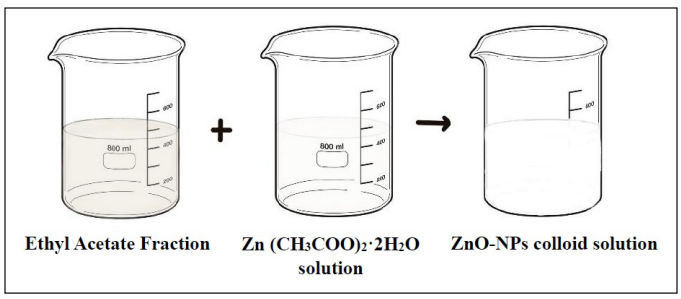

Figure 1. Scheme of the synthesis of nanoparticles by using white frangipani leaves (*P. Alba* L.).

Antimicrobial activity test of antidandruff shampoo

An antibacterial activity test of shampoo was used to determine whether the variation of the volume of ZnO-NPs 0.15-M *P. alba* in the form of shampoo still provided antibacterial effects against *S. aureus* using a well diffusion method; 50 µl of ZnO-NPs 0.15-M *P. alba* shampoo was inserted into the well. Comparison used for the negative control used a shampoo base without the addition of extract and the positive control used shampoo with the addition of 10-ppm tetracycline.

RESULTS AND DISCUSSION

Extraction and fractionation of white frangipani leaves

The crude ethanol extract of white frangipani leaves was obtained in the amount of 45.43 g, and the percentage yielded 15.14%. The crude ethanol extract was then fractionated with n-hexane, ethyl acetate, and ethanol solvent until the yield n-hexane fraction was obtained as much as 15.11%, ethyl acetate fraction 8.83%, and ethanol fraction 53.77%. Different solvents were used to dissolve the secondary metabolites based on their polarity. Polar solvents can dissolve secondary metabolites such as polyphenols, flavonoids, alkaloids, tannins, saponins, steroids, and terpenoids [17]. Meanwhile, semipolar and nonpolar solvents can dissolve secondary metabolites such as flavonoids, saponins, alkaloids, steroids, and triterpenoids [18].

Antimicrobial activity test of extract and fraction of white frangipani leaves

The result of the antimicrobial activity test is shown in Figure 2 that the highest inhibition zone diameter was observed with the ethyl acetate fraction of 1.81 ± 0.42 mm, followed by ethanol extract 0.52 ± 0.18 mm, ethanol fraction 0.46 ± 0.08 mm, n-hexane fraction 0.30 ± 0.11 mm, and aquadest 0.00 ± 0.00 mm. The antifungal activity test showed the highest inhibition zone diameter at a fraction of ethyl acetate of 1.71 ± 0.63 mm, followed by ethanol extract of 0.64 ± 0.05 mm, n-hexane fraction of 0.54 ± 0.11 mm, ethanol fraction of 0.44 ± 0.76 mm, and aquadest of 0.00 ± 0.00 mm. There were four categories of inhibition zone diameter: very strong (inhibition zone > 20 mm), strong (inhibition zone 10–20 mm), medium (inhibition zone 5–10 mm), and low (inhibition zone < 5 mm) [19]. Based

Table 1. Antidandruff shampoo formulation.

Ingredients	F1	F2	F3	F4	F5
Sodium Lauryl Sulfate (SLS) (g)	10	10	10	10	10
Carboxymethyl cellulose (CMC) (g)	1.5	1.5	1.5	1.5	15
Cocamide diethanolamine (Cocamide DEA) (g)	4	4	4	4	4
Propyl paraben (g)	0.2	0.2	0.2	0.2	0.2
Citric acid (g)	0.15	0.15	0.15	0.15	0.15
Aquades (ml)	80	80	80	80	80
Menthol (ml)	5	5	5	5	5
ZnO-NPs 0,15 M *P. alba* (ml)	0	1	5	10	0
Tetracycline (ml)	0	0	0	0	1

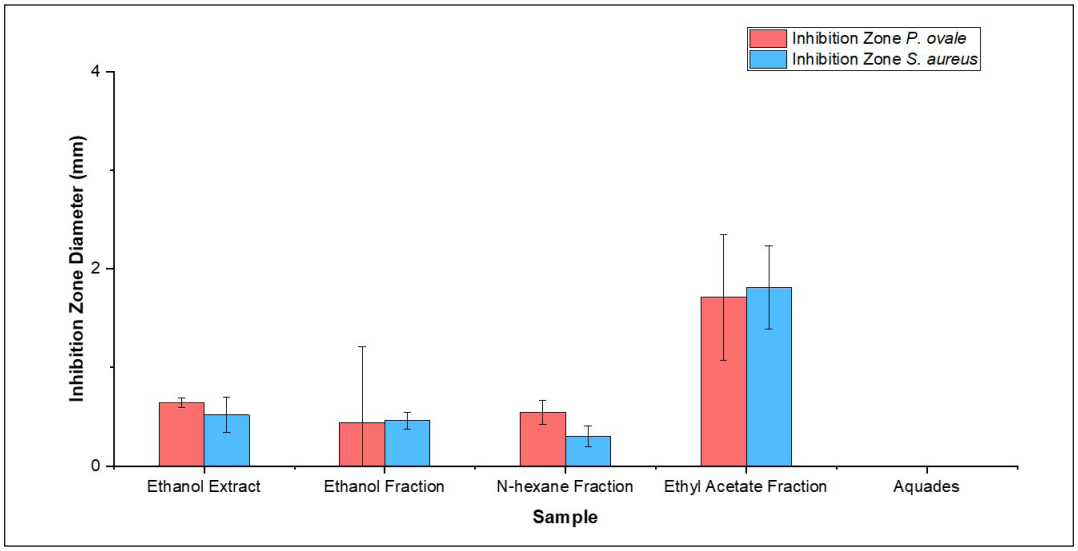

Figure 2. Inhibition zone diameter antimicrobial activity of extract and fraction of white frangipani leaves (*P. alba* L.).

on the one-way ANOVA result, the antibacterial activity test showed a *p*-value of 0.000 (< 0.05), and the antifungal activity test showed a *p*-value of 0.049 (< 0.05).

The antimicrobial activity test extract and fraction of white frangipani leaves (*P. alba* L.) against *S. aureus* and *P. ovale* are shown in Figure 2. Therefore, it can be concluded that there was a different correlation between the extract and the fraction that inhibited microbial growth. The test was continued with Duncan's multiple range test (DMRT) to determine the most significant difference between the extract and the fraction. The result from DMRT showed that the inhibition zone diameter was the most important difference in the ethyl acetate fraction. The ethyl acetate fraction has the largest inhibition zone diameter because there are secondary metabolite compounds with antimicrobial characteristics, such as terpenoids, flavonoids, alkaloids, saponins, and phenol [20]. Secondary metabolite compounds can disrupt the microbe's peptidoglycan so that the cell membrane does not form and the microbial cells are dead. Alkaloid compounds have the ability to distract bacterial peptidoglycan components so that the cell membrane is not formed and the bacteria cell dies. Flavonoid compounds work by spoiling the cell membrane of microbes, which can bind with DNA to inhibit the growth of microbes. Saponin compounds work by decreasing the surface tension of the cell that can easily penetrate antibacterial compounds due to the bacterial cell permeability decreasing continuously until the bacterial cell breaks and dies. Terpenoid compounds work by reacting with protein transmembrane, which caused the cell membrane less selectively permeable and turned the bacterial cell become lack of nutrition due to the existence of antibacterial compound inside of the cell [21]. The secondary metabolites of *P. alba* L. offered antimicrobial properties to inhibit the growth of microbes that contribute to dandruff. Besides that, the antioxidant activity of *P. alba* L. could be applied as an oxidative stress mitigation agent on the scalp [17]. To enhance the effectiveness of its antibacterial activity, the ethyl acetate fraction was used to synthesize ZnO-NPs and applied in shampoo formulation.

Phytochemical test of ethyl acetate fraction of white frangipani leaves

A phytochemical test determined the secondary metabolite compounds that could inhibit *S. aureus* and *P. ovale* growth at ethyl acetate fraction of white frangipani leaves (*P. alba* L.) [11]. The results of the phytochemical test are shown in Table 2.

Synthesis of zinc oxide nanoparticles

Zinc oxide nanoparticles were synthesized by adding sodium hydroxide to the ethyl acetate fraction of white frangipani leaves that were homogenized with $Zn(CH_3COO)_2{\cdot}2H_2O$ precursor at different concentrations (0.05 M, 0.10 M, and 0.15 M). Subsequently, they were constantly mixed until the nanoparticles formed [22]. Sodium hydroxide was then added to increase the alkalinity of the liquid. Based on [23], ZnO-NPs could be formed very well at pH 7 and precursor concentration of 0.15 M. ZnO-NPs have formed as defined by white pale colloids [24]. The reaction involved in this process is as follows:

(1) $Zn(CH_3COO)_2.2H_2O + 2NaOH \rightarrow Zn(OH)_2 + 2CH_3COONa + 2H_2O$

Table 2. Phytochemical test result of ethyl acetate fraction white frangipani leaves (*P. alba* L.).

Compound	Identification	Color	Result
Polyphenol	Green, Red, Blue, Purple, Black	Red maroon	Positive (+)
Flavonoid	Yellow	Yellow	Positive (+)
Tannins	Colloids	Clear yellow	Negative (-)
Saponins	Stable foam ± 1.5 cm until 30 minutes	Stable foam ± 1.5 cm until 30 minutes	Positive (+)
Alkaloids	Colloids	White colloids	Positive (+)
Steroids	Green—Blue	Red brownies	Negative (-)
Terpenoids	Red—Purple	Red brownies	Positive (+)

(2) $Zn(OH)_2 + 2H_2O \rightleftharpoons Zn^{2+} + 2OH^- + 2H_2O \rightleftharpoons [Zn(OH)_4]^{2-}$
(3) $[Zn(OH)_4]^{2-} \leftrightarrow ZnO_2^{2-} + 2H_2O$
(4) $ZnO_2^{2-} + 2H_2O \leftrightarrow ZnO + 2OH^-$ [25]

The formation of ZnO-NPs began at the nucleus formation of ZnO. When the liquid's alkalinity increased, ZnO-NPs started to form, which was identified by the color change in the liquid, becoming white colloids. Half of the colloids becomes Zn^{2+} ions and OH^- ions as ZnO formers, as shown in reaction [3]. $[Zn(OH)_4]^{2-}$ functions as the growth of fundamental units of the Np-ZnO structure [26]. Then, after Zn^{2+} ions and OH^- ions achieve the right degree of saturation of ZnO, the nucleus of ZnO-NPs is formed by the fourth reaction [27]. ZnO-NPs included were then tested for antimicrobial activity, and ZnO-NPs with the highest antimicrobial activity were then characterized using FTIR, SEM-EDX, PSA, and XRD.

Antimicrobial activity of zinc oxide nanoparticles

The chart is shown in Figure 3 that ZnO-NPs control has inhibition zone diameter antibacterial activity as wide as 0.72 ± 0.21 mm, ZnO-NPs 0.05-M *P. alba* 5.76 ± 0.53 mm, ZnO-NPs 0.10-M *P. alba* 6.38 ± 0.55 mm, ZnO-NPs 0.15-M *P. alba* 8.50 ± 0.77 mm, tetracycline 20.29 ± 1.67 mm, and aquadest 0.00 ± 0.00 mm. Then, the antifungal activity test showed the inhibition zone diameter of ZnO-NPs control as big as 0.53 ± 0.20 mm, ZnO-NPs 0.05-M *P. alba* 0.65 ± 0.05 mm, ZnO-NPs 0.10-M *P. alba* 1.30 ± 0.17 mm, ZnO-NPs 0.15-M *P. alba* 2.7 ± 0.17 mm, ketoconazole 6.89 ± 0.69 mm, and aquadest 0.00 ± 0.00 mm. One-way ANOVA showed a *p*-value of inhibition zone diameter of antibacterial and antifungal activity of 0.000 (<0.05). Thus, it can be concluded that there was a different correlation between the ZnO-NPs that were used to inhibit microbial growth. Following the one-way ANOVA test result, the sequence progressed to DMRT. It showed that the inhibition zone diameter with a really different correlation was ZnO-NPs 0.15-M *P. alba*.

Antimicrobial activity test zinc oxide nanoparticles against *S. aureus* and *P. ovale* are shown in Figure 4. This result was the same as that in [28], which showed a significant improvement in the size of inhibition zone diameter along with the improvement in precursor variation in the formation of nanoparticles caused by the size of nanoparticles formed. The smaller the ZnO-NP size, the easier it penetrates the microbial cell membrane [29]. Growth of microbes by ZnO-NPs was inhibited by spoiling the cell membrane by releasing Zn^{2+} ions. Zn^{2+} ions interacted with thiol compounds at the cell membrane of the microbes, which could increase the membrane permeability. Thus, the cell membrane is oxidized, and the microbe's cell is dead [25].

Characterization of zinc oxide nanoparticles

Fourier transform infrared

As shown in Figure 5, the ethyl acetate fraction of white frangipani leaves showed band-broadening absorption at the wavelength 3394.72 cm^{-1} with strong vibration intensity that revealed the existence of the O–H group, which came from polyphenols, flavonoids, alkaloids, terpenoids, and saponins.

There was a strain of C–H aliphatic group at a wavelength of 2,924.09 cm^{-1}, a C=O group at wavelength 1,689.64 cm^{-1} with sharp strain absorption, a C=C group at a wavelength of 1,597.06 cm^{-1} with low intensity, and a strain of C–O alcohol group at a wavelength of 1,273.02 cm^{-1}. Based on the FTIR spectrum interpretation, the ethyl acetate fraction contains O–H, C–O alcohol, C–H aliphatic, C=C, and C=O functional groups, which came from secondary metabolite compounds, such as terpenoids, flavonoids, alkaloids, and saponins [30, 31].

X-ray diffraction

Peaks at 31.70°, 34.37°, 36.18°, 47.51°, 56.51°, 62.75°, and 67.90° angles are related to (100), (002), (101), (102), (110), (103), and (201). ZnO-NPs control showed diffraction peaks at 31.60°, 34.27°, 36.12°, 47.34°, 56.54°, 62.72°, and 67.75° angles, which are related to (100), (002), (101), (102), (110), (103), and

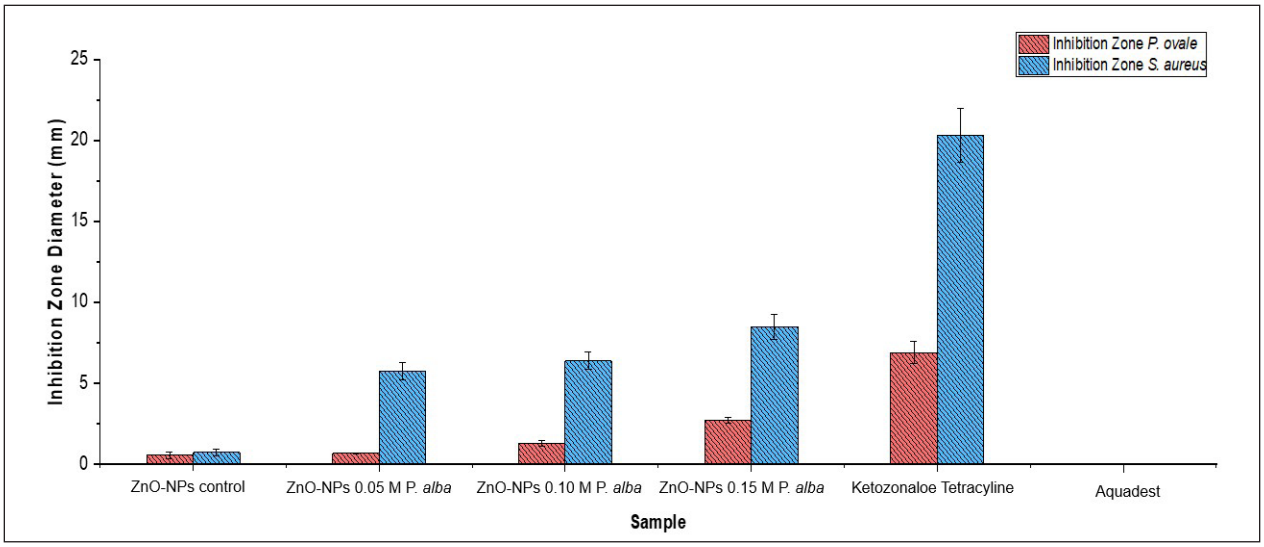

Figure 3. Inhibition zone diameter antimicrobial activity of ZnO-NPs.

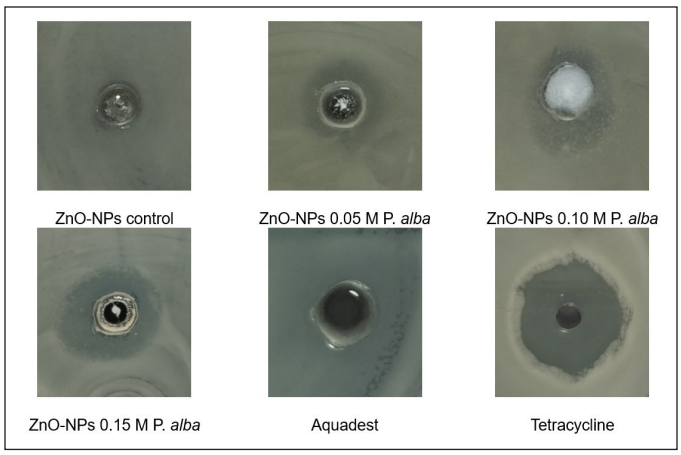

Figure 4. Antimicrobial activity test zinc oxide nanoparticles against *S. aureus* and *P. ovale.*

(201), respectively. Every angle diffraction peak of the ZnO-NPs 0.15-M *P. alba* and ZnO-NPs control is similar to the Joint Committee on Powder Diffraction Standards Card No. 36-1451, which, based on those patterns, showed that ZnO-NPs' sample has a hexagonal wurtzite structure [7]. This hexagonal structure was similar to the morphology observed in the SEM analysis. The XRD pattern is shown in Figure 6.

Particle size analyzer

Based on the size distribution of ZnO-NPs 0.15-M *P. alba* in Table 3, the result of ethyl acetate fraction of white frangipani leaves sample has a diameter of 869 nm within 36.4% volume and 5840 nm within 64.6% volume, and ZnO-NPs 0.15-M *P. alba* has diameter 6.63 nm within 10.3% volume and 259.5 nm within 89.7% volume. ZnO-NPs control has a diameter of 493 nm within 43.6% volume and 1,569 nm within 56.4% volume. ZnO-NPs control and ZnO-NPs 0.15-M *P. alba* had different nanoparticle sizes. It was caused by adding ethyl acetate fraction, which functioned as a capping agent that could reduce the particle size. The existence of a capping agent could transform the synthesized compound to become more stable and minimize the aggregation process; thus, it could convert the particle diameter of the synthesized compound into a nanoparticle [32].

Scanning electron microscope-energy dispersive X-ray

Figure 7 shows the morphology of ZnO-NPs control and ZnO-NPs 0.15-M *P. alba*. ZnO-NPs control had a spherical morphology and particle aggregation. A spherical shape was formed during ZnO-NPs synthesis using $Zn(CH_3COO)_2 \cdot 2H_2O$ as the precursor and the aquadest as the solvent [33]. ZnO-NPs 0.15-M *P. alba* showed a needle rod shape and particle aggregation at the edge of the rod. Aggregation occurs at the ZnO-NPs 0.15-M *P. alba* and ZnO-NPs control because the synthesis process has been held using an aqueous solvent as the base media, and particle aggregation usually occurs during this synthesis process [34]. The morphological differences between ZnO-NPs control and ZnO-NPs 0.15-M *P. alba* were due to adding the ethyl acetate fraction to ZnO-NPs 0.15-M *P. alba*. ZnO-NPs with rod morphology could appear if the solvent used in synthesizing contained ethyl acetate, formic, or chloride [35]. The appearance of a needle shape at the edge of the rod was due to secondary metabolite compounds already existing in the ethyl acetate fraction. The rod morphology was formed first, followed by the needle morphology along

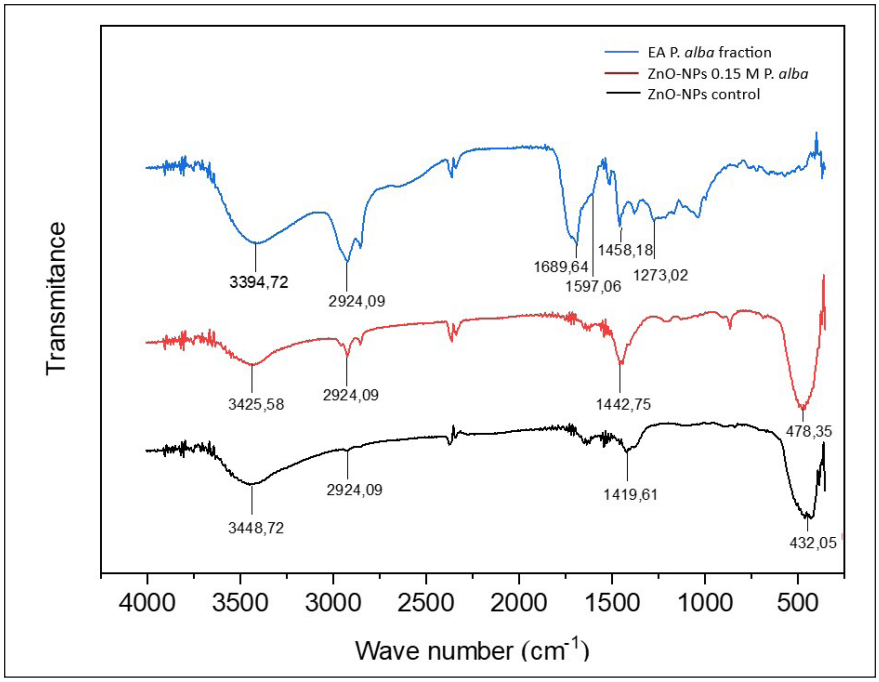

Figure 5. Analysis FTIR result of ethyl acetate fraction of white frangipani leaves (blue), ZnO-NPs 0.15-M P. *alba* (red), and ZnO-NPs control without fraction addition (black).

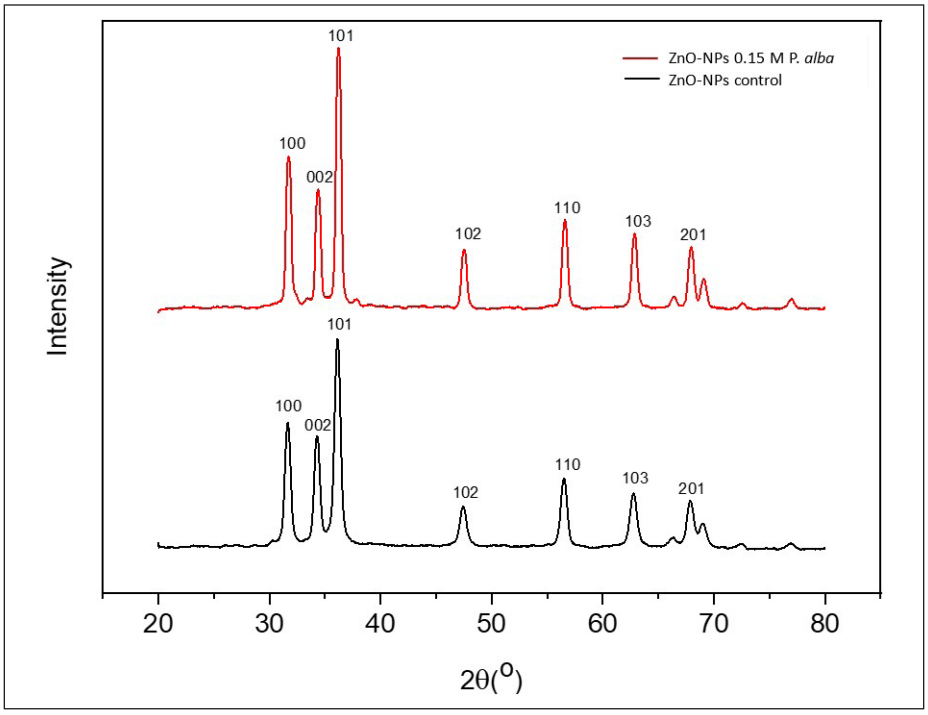

Figure 6. Analysis XRD result of ZnO-NPs 0.15-M *P. alba* (red) and ZnO-NPs control without fraction addition (black).

Table 3. Analysis PSA result.

Sampel	Diameter (nm)	Volume (%)	Diameter (nm)	Volume (%)
Ethyl acetate fraction	869	36.4%	5840	63.6%
ZnO-NPs 0,15 M *P. Alba*	6.63	10.3%	259.5	89.7%
ZnO-NPs control	493	43.6%	1568	56.4%

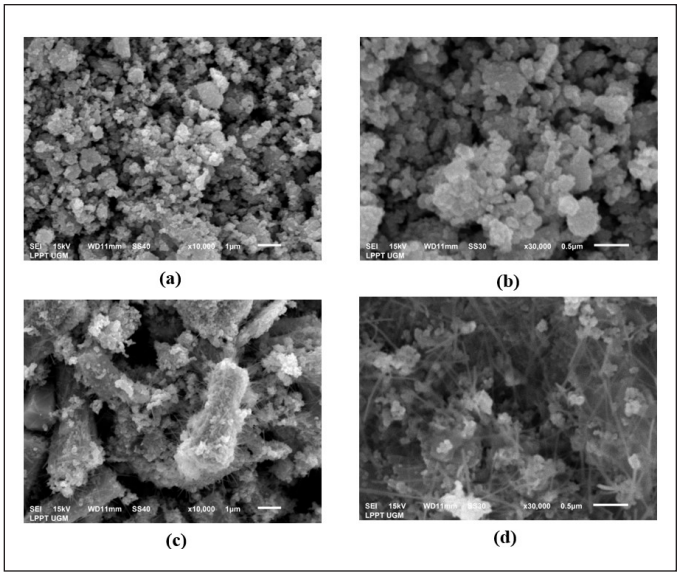

Figure 7. Analysis SEM result (a) ZnO-NPs control enlargement × 10.000 1 µm, (b) ZnO-NPs control enlargement × 30.000 0.5 µm, (c) ZnO-NPs 0.15-M *P. alba* enlargement × 10.000 1 µm, and (d) ZnO-NPs 0.15-M *P. alba* enlargement × 30.000 0.5 µm.

the edge of the rod. This mechanism is based on an epitaxial process, where there are two-way processes of the bundle lone crystalline [36]. Even though the ethyl acetate fraction that was added during the synthesis of ZnO-NPs was not too much (1:9), its existence could significantly affect the morphology of the nanoparticles. The analysis EDX result of ZnO-NPs 0.15-M *P. alba* is shown in Figure 8.

The purity and composition of ZnO-NPs 0.15-M *P. alba* showed a strong energy signal at the zinc (Zn) peak and a weak energy signal at the oxygen (O) peak. The absorption type of ZnO-NPs obtained is similar to [33], predominantly in the absorption range of 1 keV and weak at the absorption range between 8 and 10 keV. The percentage compositions of the EDX analysis results are presented in Table 4.

Element Zn has an atomic percentage of 50.81% and a mass percentage of 80.84%. Element O has an atomic percentage of 49.19% and a mass percentage of 19.16%. Based on the data above, the obtained ZnO-NPs have a high purity.

Based on the characterization result, the FTIR analysis showed that there was sharp shifting within the wavelength of 2924.09 in ZnO-NPs 0.15-M *P. alba*, which indicates the existence of secondary metabolites that came from the ethyl acetate fraction of *P. alba*. Related to the XRD analysis, the structure of ZnO-NPs 0.15 M *P. alba* has shown hexagonal wurtzite zinc oxide nanoparticles [32]. The result of PSA analysis showed that the ZnO-NPs 0.15 M *P. alba* has a nanoparticle size at 6.63 nm within 10.3% volume of solution. The morphology of the ZnO-NPs 0.15-M *P. alba* was shown in needle rod shape by using the SEM-EDX analysis.

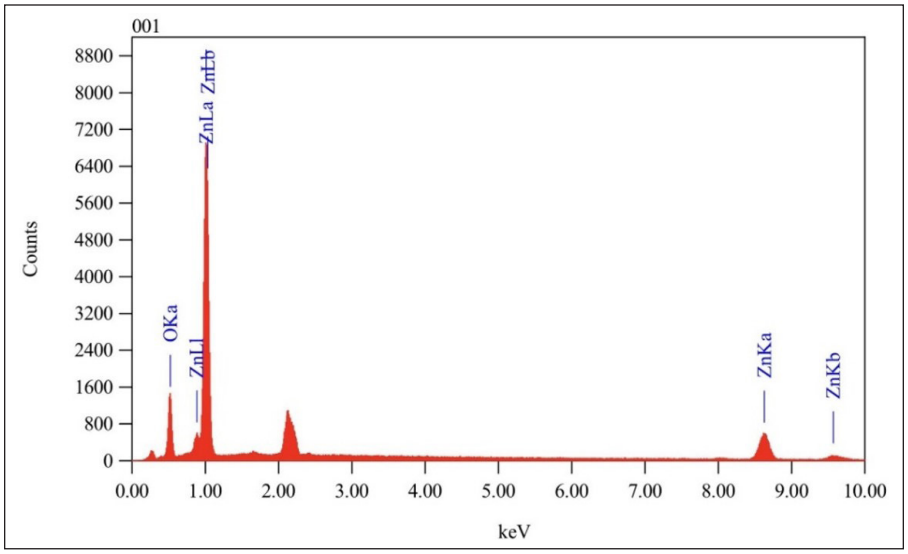

Figure 8. Analysis EDX result of ZnO-NPs 0.15-M *P. alba.*

Table 4. Composition analysis EDX of ZnO-NPs 0.15 M P. *alba.*

Element	keV	Mass%	Atom%
Zn	8.630	80.84	50.81
O	0.525	19.16	49.19
Total		100.00	100.00

Formulation and characterization of shampoo

Shampoo formulation labeled F1 served as a negative control, F2–F4 contained variations of ZnO-NPs, and F5 acted as a positive control with the addition of tetracycline. Shampoo formulations were characterized over 15 days to monitor their consistency.

According to the Indonesian National Standard (SNI) 06-2692-1992, the acceptable pH range for shampoo formulations is 5.0–9.0. Based on Figure 9, the pH value increased with the addition of varying volumes of 0.15-M *P. alba* ZnO-NPs and exhibited minor or stable fluctuations over the storage period. Research by [37] showed that the addition of active compounds in shampoo formulations could elevate pH values toward neutrality and contribute to maintaining pH stability during storage. Based on the data, the pH values of the prepared shampoos were within the acceptable range.

Water content of the shampoo was measured to determine the quantity of water present in the formulation. Shampoos with water content exceeding 95.5% fall outside the threshold established by SNI 06-2692-1992. Based on Figure 10, observed water content tended to increase with the addition of active compounds and fluctuated during storage. However, the water content remained below the standard limit, qualifying the formulations as suitable shampoos.

An emulsion stability test was conducted to evaluate the durability of the shampoo formulation during storage. Higher stability indicates a longer shelf life for the shampoo. Overall, the emulsion stability of the formulations, based on varying volumes of 0.15-M *P. alba* ZnO-NPs in Figure 11,

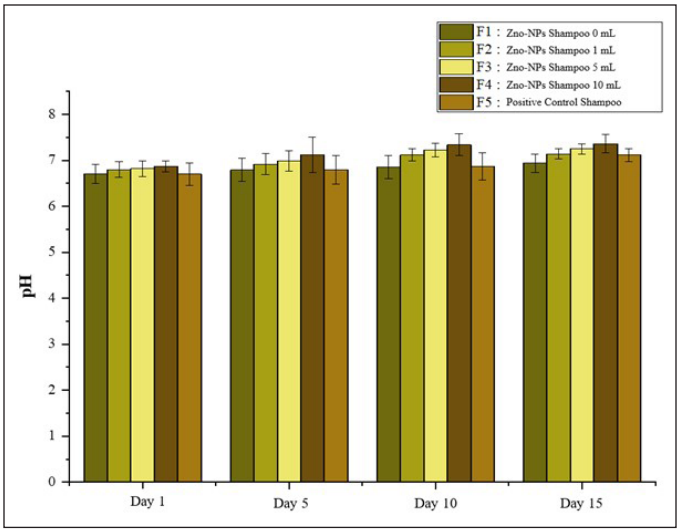

Figure 9. pH of formulation shampoo.

showed minor fluctuations, with no significant differences between formulations. Shampoo with high foam stability is considered ideal for use.

Foam stability of the formulations, influenced by variations in the volume of 0.15-M *P. alba* ZnO-NPs, demonstrated fluctuating trends shown in Figure 12 but generally decreased as the volume increased. Regarding storage duration, foam stability showed a decline on day 5, followed by an increase on day 10. Shampoo formulations with high foam stability are ideal for use. According to [38], shampoos that produce stable and abundant foam can clean dirt more effectively. Stable foam is generated by surfactants with amphiphilic properties, allowing impurities such as excess sebum and attached dust to dissolve within the hydrophobic structure of the surfactant. When rinsed with water, these impurities are then carried away and dissolved into the hydrophilic structure of the surfactant [16].

According to SNI 06-2692-1992, good shampoo formulations should have 0% free alkali content. The high alkali content in shampoo can increase its pH, rendering it alkaline, which may lead to dry, coarse, and brittle hair. The analysis of free alkali content in the formulations with varying volumes of 0.15-M *P. alba* ZnO-NPs consistently showed 0% across the tests conducted on days 5, 10, and 15. This aligns with the reference by SNI 06-2692-1992 confirming that the shampoo formulations are of good quality and do not damage hair.

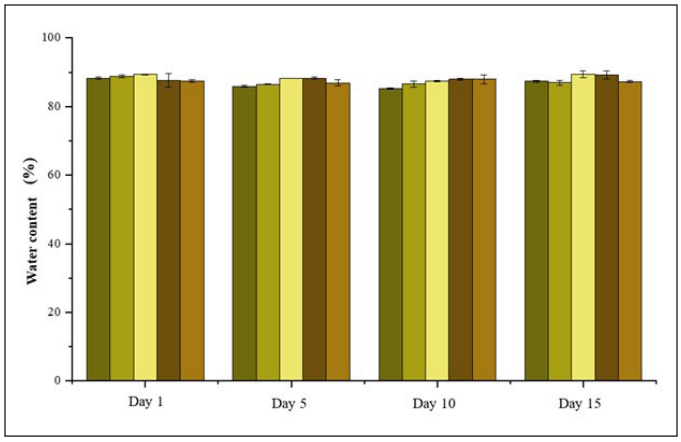

Figure 10. Water content of formulation shampoo.

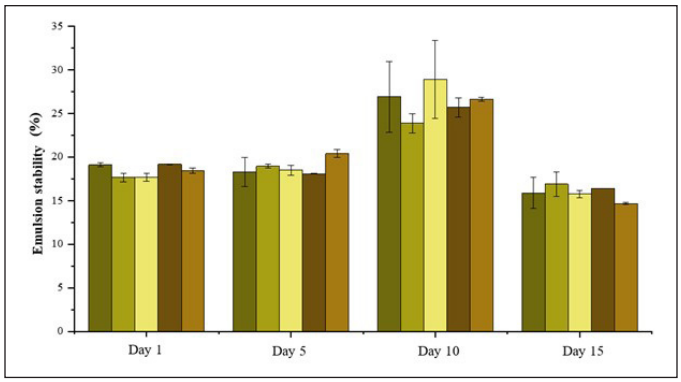

Figure 11. Emulsion stability of formulation shampoo.

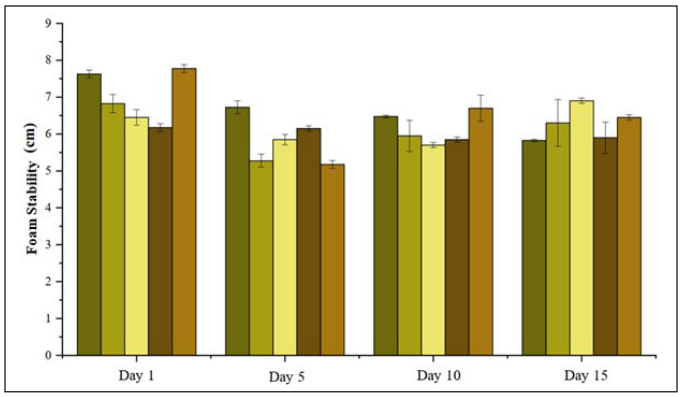

Figure 12. Foam stability of formulation shampoo.

High viscosity made shampoo hard to be applied on hair. Low viscosity caused shampoo to not be stable. The viscosity of the formulations in Figure 13 tended to decrease with the addition of increasing volumes of 0.15-M *P. alba* ZnO-NPs. However, over the storage period, the viscosity significantly increased by day 15. The decrease in viscosity is associated with the added volume of 0.15-M *P. alba* ZnO-NPs, as higher volumes tend to reduce the viscosity of the formulation [39].

Antibacterial activity test of shampoo

The antibacterial activity of the shampoo formulations was tested to evaluate their ability to inhibit bacterial growth, specifically targeting *S. aureus*, which can overpopulate the scalp and cause dandruff.

The results, as shown in Figure 14, indicate a strong inhibition zone diameter for F1, measuring 17.43 ± 0.43 mm on day 1 and 20.67 ± 0.45 mm on day 15. This is attributed to the addition of propylparaben, which functions as an antibacterial agent, extending the shampoo's shelf life [40]. However, shampoo formulations containing 0.15-M *P. alba* ZnO-NPs exhibited superior antibacterial activity compared to the negative control shampoo. Inhibition zone diameters of the shampoos with 0.15-M *P. alba* ZnO-NPs were greater than that of the negative control. Specifically, F1 exhibited inhibition zone diameters of

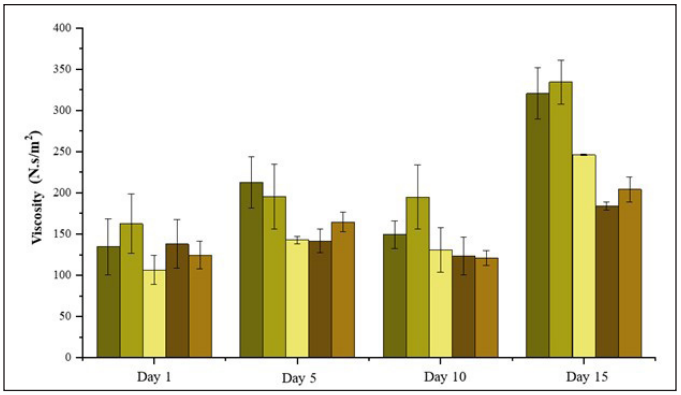

Figure 13. Viscosity of formulation shampoo.

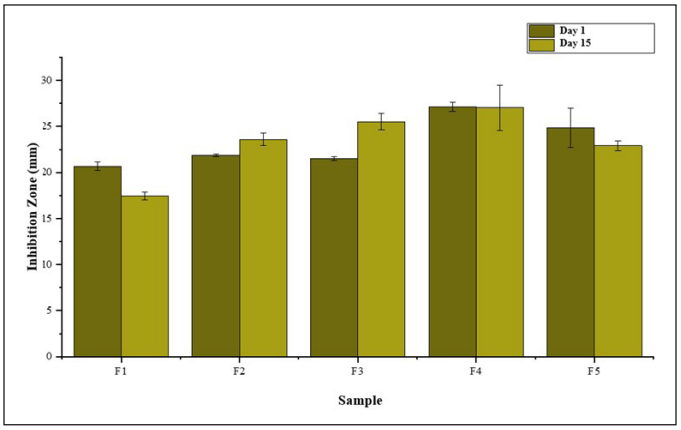

Figure 14. Antibacterial zone of formulation ZnO-NPs M *P. alba* shampoo.

17.43 ± 0.42 mm on day 1 and 20.67 ± 0.45 mm on day 15; F2 exhibited 23.59 ± 0.66 mm on day 1 and 21.87 ± 0.16 mm on day 15; F3 exhibited 25.63 ± 0.87 mm on day 1 and 21.49 ± 0.21 mm on day 15; F4 exhibited 27.04 ± 2.46 mm on day 1 and 27.12 ± 0.49 mm on day 15; and F5 exhibited 22.91 ± 0.52 mm on day 1 and 24.83 ± 2.14 mm on day 15.

Shampoo with the most optimal antibacterial activity was F4, with inhibition zone diameters of 27.04 ± 2.46 mm on day 1 and 27.12 ± 0.49 mm on day 15. This enhanced activity is likely due to the higher content of 0.15-M *P. alba* ZnO-NPs in the formulation. The higher the concentration of active compounds in the shampoo, the greater its ability to diffuse into bacterial cells and inhibit their growth [41].

Inhibition zone data were analyzed using one-way ANOVA to determine significant differences in the antibacterial activity of the shampoos against *S. aureus*. The one-way ANOVA results showed a *p*-value of 0.000 (<0.05) both on days 1 and 15, indicating significant differences among the shampoos in inhibiting bacterial growth. A subsequent DMRT was performed to identify which shampoo formulations exhibited the most significant differences. DMRT results highlighted that the 10-ml *P. alba* ZnO-NPs shampoo showed the most significant inhibition zone, measuring 27.04 ± 2.46 mm on day 1 and 27.12 ± 0.49 mm on day 15. Shampoo formulations with the addition of 0.15-M *P. alba* ZnO-NPs as an active ingredient demonstrated significant differences in their ability to inhibit the growth of *S. aureus*, with F4 being the most effective.

CONCLUSION

Variation of precursor $Zn(CH_3COO)_2 \cdot 2H_2O$ concentration toward ZnO-NPs formation has the highest antimicrobial activity at ZnO-NPs 0.15-M *P. alba* with the smallest distribution particle of 6.63 nm. The FTIR analysis of ZnO-NPs 0.15-M *P. alba* showed O–H functional groups at a wavelength of 3,425.58 cm^{-1}, C–H aliphatic at 2,924.09 cm^{-1}, C–O alcohol at 1,273.02 cm^{-1}, and zinc oxide nanoparticles group at 478.35 cm^{-1}. XRD analysis results showed the structural similarity of the ZnO-NPs 0.15-M *P. alba* with ZnO-NPs control, which was hexagonal wurtzite. Analysis of PSA results showed that the size of ZnO-NPs 0.15-M *P. alba* nanoparticles was as big as 6.63 nm within 10.3% volume. SEM-EDX analysis showed that the needle rod morphology of ZnO-NPs 0.15-M *P. alba* and the composition consisted of Zn 80.84% and O 19.16%. Antibacterial analysis of shampoo with the addition of 0.15-M *P. alba* ZnO-NPs demonstrated more optimal antibacterial activity compared to the shampoo formulations without the addition of 0.15-M *P. alba* ZnO-NPs. This study has shown a significant result, yet it has limitations in the optimum result of antibacterial activity. Thus, the next study needed to be focused on optimizing the chemical structure of the ZnO-NPs to accelerate the antimicrobial activity.

ACKNOWLEDGMENT

The author would like to thank the Jenderal Soedirman University.

AUTHOR CONTRIBUTIONS

All authors made substantial contributions to conception and design, acquisition of data, or analysis and interpretation of data; took part in drafting the article or revising it critically for important intellectual content; agreed to submit to the current journal; gave final approval of the version to be published; and agree to be accountable for all aspects of the work. All the authors are eligible to be an author as per the International Committee of Medical Journal Editors (ICMJE) requirements/guidelines.

FINANCIAL SUPPORT

This work is funded by the Research Grant of 'Riset Dasar Jenderal Soedirman University': contract number 27.106/UN23.37/PT.01.03/II/2023.

CONFLICTS OF INTEREST

The authors report no financial or any other conflicts of interest in this work.

ETHICAL APPROVALS

This study does not involve experiments on animals or human subjects.

DATA AVAILABILITY

All data generated and analyzed are included in this research article.

PUBLISHER'S NOTE

This journal remains neutral with regard to jurisdictional claims in published institutional affiliation.

REFERENCES

1. Mas-Ud AM, Ali RM, Hasan ZSM, Islam AM, Hasan FM, Islam AM, *et al.* Molecular detection and biological control of human hair dandruff causing microorganism *Staphylococcus aureus*. J Pure Appl Microbiol. 2020;14(1):147–56.
2. Sari NKY, Sumadewi NLU, Deswiniyanti NW, Putra DGIP. Efektivitas anti fungi Ekstrak Bunga Kamboja Putih (*Plumeria acuminata*) Menghambat Pertumbuhan *Candida albicans*. J Media Sains. 2020;4(1):21–4.
3. Ningsih DR, Purwati P, Zusfahair Z, Nurdin A. Potensi Ekstrak Daun Kamboja (*Plumeria alba* L.) Sebagai Antibakteri dan Identifikasi Golongan Senyawa Bioaktifnya. Molekul. 2014;9(11):101–9.
4. Sirelkhatim A, Mahmud S, Seeni A, Kaus NHM, Ann LC, Bakhori SKM, *et al.* Review on zinc oxide nanoparticles: antibacterial activity and toxicity mechanism. Nano-Micro Lett. 2015;7(3):219–42.
5. Hussain I, Singh NB, Singh A, Singh H, Singh SC. Green synthesis of nanoparticles and its potential application. Biotechnol Lett. 2016;38(4):545–60.
6. Mirzaei H, Darroudi M. Zinc oxide nanoparticles: biological synthesis and biomedical applications. Ceram Int. 2017;43(1):907–14.
7. Kolodziejczak-Radzimska A, Jesionowski T. Zinc oxide from synthesis to application: a review. Materials (Basel). 2014;7(4):2833–81.
8. Islam F, Shohag S, Uddin MJ, Islam MR, Nafady MH, Akter A, *et al.* Exploring the journey of zinc oxide nanoparticles (ZnO-NPs) toward biomedical applications. Materials (Basel). 2022;15(6):1–31.
9. Wardhani LK, Sulistyani N. Uji Aktivitas Antibakteri Ekstrak Etil Asetat Daun Binahong (*Anredera scandens* (L.) Moq.) Terhadap *Shigella flexneri* Beserta Profil Kromatografi Lapis Tipis. J Ilm Kefarmasian. 2012;2(1):1–16.
10. Padamani E, Ngginak J, Lema AT. Analisis Kandungan Polifenol Pada Ekstrak Tunas Bambu Betung (*Dendrocalamus asper*). Bioma J Biol Dan Pembelajaran Biol. 2020;5(1):52–65.
11. Lestari D, Fitriani D, Anngraeni S. Skrining Fitokimia dan Uji Aktivitas Antibakteri Fraksi Etil Asetat dan n-Heksana dari Daun

Mangga Kasturi (*Mangifera casturi* Kosterm.). KOVALEN J Ris Kim. 2021;7(3):227–33.
12. Sulistyarini I, Sari A, Tony D, Wicaksono A. Skrining Fitokimia Senyawa Metabolit Sekunder Batang Buah Naga (*Hylocereus polyrhizus*). J Ilm Cendekia Eksakta. 2020;5(1):56–62.
13. Malonda TC, Yamlean PVY, Citraningtyas G. Formulasi Sediaan Sampo Antiketombe Ekstrak Daun Pacar Air (*Impatiens balsamina* L.) dan Uji Aktivitasnya Terhadap Jamur *Candida albicans* ATCC 10231 Secara In Vitro. Pharmacon J Ilm Farm. 2017;6(4):97–109.
14. Suryani A, Sailah I, Hambali E. Teknologi Emulsi. Bogor, Indonesia: IPB; 2002.
15. Annisanur A, Musfiroh I. Evaluation of shampoo by quality control: review. Indones J Pharm. 2022;4(2):267–76.
16. Lumbantoruan P, Yulianti E. Pengaruh Suhu terhadap Viskositas Minyak Pelumas (Oli). J Sainmatika. 2016;13(2):26–34.
17. Anggoro AB, Wijaya EL, Elisa N. (Antioxidant activity of extracts and fractions of white cambodian leaves (*Plumeria alba* L.) against 1,1-Diphenylpicrylhydrazine. J Ilm SAINS. 2022;22(2):111–7.
18. Anjaswati D, Pratimasari D, Nirwana AP. Perbandingan Rendemen Ekstrak Etanol, Fraksi n-Heksana, Etil Asetat, dan Air Daun Bit (*Beta vulgaris* L.) Menggunakan Fraksinasi Bertingkat. J Pharm Sci Technol. 2021;3(1):19–28.
19. Syarifuddin A, Wijayatri R, Kurniawan IF, Agusta HF. Penentuan Kurva Pertumbuhan dan Aktivitas Antibakteri dari Isolat Ekstrak Etil Asetat Bakteri (Te.325) terhadap *Staphylococcus aureus* dan *Escherichia coli*. J Ilmu Kefarmasian Indones. 2022;20(2):252–8.
20. Rasmawati NL, Fatmawati NND. Uji Daya Hambat Ekstrak Etil Asetat Daun Kamboja (*Plumeria rubra* var. acutifolia) Terhadap Pertumbuhan Bakteri methicillin resistant *Staphylococcus aureus* Secara *in vitro*. J Med Udayana. 2020;9(4):53–7.
21. Cahyadi J, Satriain GI, Gusman E, Weliyadi E, Sabri. Phytochemical screening of mangrove fruit extract (*Sonneratia alba*) as natural feed bioenrichment *Artemia salina*. J Borneo Saintek. 2018;1(3):33–9.
22. Romadhan MF, Suyatma NE, Taqi FM. Synthesis of ZnO nanoparticles by precipitation method with their antibacterial effect. Indones J Chem. 2016;16(2):117–23.
23. Arifin FS, Nazriati. Biosintesis dan Karakterisasi Nanopartikel Seng Oksida (ZnO-NPs) Menggunakan Ekstrak Daun Kenitu (*Chrysophyllum cainito* L.). J Tek Kim USU. 2022;11(2):56–63.
24. Yunita Y, Nurlina N, Syahbanu I. Sintesis nanopartikel zink oksida (ZnO) dengan Penambahan Ekstrak Klorofil sebagai Capping Agent. POSITRON. 2020;10(2):123–30.
25. Prasetya YA, Nisyak K, Hisbiyah A. Aktivitas antibakteri dan antibiofilm nanokomposit seng Oksida-Perak (ZnO-Ag) dengan Minyak Cengkeh terhadap *Pseudomonas aeruginosa*. J Bioteknol Biosains Indones. 2021;8(2):196–207.
26. Osman DAM, Mustafa MA. Synthesis and characterization of zinc oxide nanoparticles using zinc acetate dihydrate and sodium hydroxide. J Nanosci Nanoeng. 2015;1(4):248–51.
27. Saragi T, Purba YR, Auffa S, Oktaviani M, Susilawati T, Risdiana, *et al.* Karakteristik Nanopartikel ZNO: Studi Efek Pelarut Pada Proses Hidrothermal. J Mater Dan Energi Indones. 2016;6(1):35–8.
28. Eskani IN, Laela E, Haerudin A, Setiawan J, Lestari DW, Isnaini, *et al.* Aplikasi Nano Partikel ZnO Secara Insitu Untuk Fungsionalisasi Antibakteri Pada Kain Batik. Din Kerajinan Dan Batik Maj Ilm. 2021;38(2):217–26.
29. Putri IE, Suyatma NE, Kusumaningrum HD. Film Edibel Antibakteri Berbasis Isolat Protein Kedelai Dengan Ekstrak Kunyit Dan Nanopartikel Seng Oksida. J Teknol dan Ind Pangan. 2018;29(1):85–92.
30. Sari KAI, Gunawan IWG, Putra KGD. Kapasitas Antioksidan Senyawa Golongan Triterpenoid Pada Daun Pranajiwa (*Euchresta horsfieldii* lesch benn). J Kim. 2015;9(1):61–6.
31. Atmoko DP, Marliana E, Erwin. Isolasi Dan Karakterisasi Senyawa Terpenoid Dari Daun *Macaranga beccariana* Merr. J Kim Mulawarman. 2018;18(1):22–6.
32. Demissie MG, Sabir FK, Edossa GD, Gonfa BA. Synthesis of zinc oxide nanoparticles using leaf extract of *Lippia adoensis* (Koseret) and evaluation of its antibacterial activity. J Chem. 2020;2020:1–9.
33. Vijayakumar S, Vaseeharan B, Malaikozhundan B, Shobiya M. Laurus nobilis leaf extract mediated green synthesis of ZnO nanoparticles: characterization and biomedical applications. Biomed Pharmacother. 2016;84(2016):1213–22.
34. Darvishi E, Kahrizi D, Arkan E. Comparison of different properties of zinc oxide nanoparticles synthesized by the green (using *Juglans regia* L. leaf extract) and chemical methods. J Mol Liq. 2019 Jul;286.
35. Dallatu YA, Shallangwa GA, Africa SN. Synthesis and growth of spherical ZnO nanoparticles using different amount of plant extract; characterization and morphology of structures. J Appl Sci Environ Manag. 2020;24(12):2147–51.
36. Tan C, Chen J, Wu XJ, Zhang H. Epitaxial growth of hybrid nanostructures. Nat Rev Mater. 2018;3:1–13.
37. Mahataranti N, Astuti IY, Asriningdhiani B. Formulasi shampo antiketombe Ekstrak Etanol Seledri (*Apium graveolens* L) dan Aktivitasnya Terhadap Jamur *Pityrosporum ovale*. J Pharm. 2012;9(2):128–38.
38. Puspitaningrum R, Fajriati I. Pengaruh Komposisi Sodium Lauryl Sulfat dalam Deterjen Kaolin Terhadap Mikroorganisme Pada Air Liur Anjing. Anal Environ Chem. 2022;7(1):21–34.
39. Gunawan A. Optimasi Formula Sampo Ekstrak Lapisan Putih Kulit Buah Semangka (*Citrullus vulgaris* Schrad) Dengan Kombinasi Hpmc Dan Sarkosyl Serta Uji Aktivitasnya Pada Jamur *Pityrosporum ovale*. J Kesehat Tujuh Belas (Jurkes TB). 2020;1(2):105–23.
40. Tjiang WM, Diah NP, Dewi K, Agus P, Prayoga A, Putu D, *et al.* Analisis Kualitatif Dan Kuantitatif Kandungan Paraben Dalam Kosmetik Hand Body Lotion. Indones J Leg Forensic Sci. 2019;9(2):89–96.
41. Taufoqurrrahman M, Pijaryani I. Uji Mutu Fisik Formula Sampo Ekstrak Kulit Markisa (*Passiflora edulis*) Sebagai Antiketombe. J Ilmu Kefarmasian. 2023;4(1):224–8.

How to cite this article:
Ningsih DR, Caroline P, Purwati P, Zusfahair Z, Riapanitra A. Green synthesis of zinc oxide nanoparticles using ethyl acetate fraction of white frangipani leaves (*Plumeria alba* L.) and its application as antidandruff shampoo. J Appl Pharm Sci. 2025;15(08):071–081. DOI: 10.7324/JAPS.2025.230314